ZIBELINE INTERNATIONAL™ PUBLISHING

ISSN: 2521-5051 (Print)
ISSN: 2521-506X (Online)
CODEN: ASMCCQ

Acta Scientifica Malaysia (ASM)

DOI: http://doi.org/10.26480/asm.02.2025.109.116

RESEARCH ARTICLE

PHYTOCHEMICAL-ASSISTED SYNTHESIS OF IRON OXIDE NANOPARTICLES FROM PICRALIMA NITIDA STEM BARK: STRUCTURAL CHARACTERIZATION AND ANTIOXIDANT PROPERTIES

Aghedo, Oscar Notoriuwa[a]*, Ogbeide, Osahon Kennedy[b] , Imafidon, Monday Idiaghe[b], Iyekowa Osaro[b]

[a] Department a Department of Science Laboratory Technology, Faculty of Life Sciences, University of Benin, Benin City, Nigeria
[b] Department of Chemistry, Faculty of Physical Sciences, University of Benin, Benin City, Nigeria
**Corresponding Author Email: Oscar.aghedo@uniben.edu*

ARTICLE DETAILS

Article History:

Received 10 July 2025
Revised 15 August 2025
Accepted 29 September 2025
Available online 03 October 2025

ABSTRACT

This study reports the green synthesis of iron oxide nanoparticles (FeONPs) using Picralima nitida stem bark extract, a plant renowned for its rich phytochemical profile. The extract served as a natural reducing and stabilizing agent, leveraging bioactive compounds such as flavonoids, alkaloids, phenolics, saponins, and tannins to mediate nanoparticle formation. The synthesized FeONPs were characterized using UV–Vis spectroscopy, FTIR, dynamic light scattering (DLS), scanning electron microscopy (SEM), and X-ray diffraction (XRD), confirming the formation of crystalline, pyramidal nanoparticles with an average size of 45.15 nm. Antioxidant activity was assessed using the DPPH radical scavenging assay, with the FeONPs showing moderate activity (IC_{50} = 1200.87 µg/mL) compared to the P. nitida extract (IC_{50} = 14.93 µg/mL) and ascorbic acid (IC_{50} = 420.55 µg/mL). These findings highlight the potential of P. nitida in green nanotechnology and suggest promising applications of FeONPs in biomedical and environmental fields due to their eco-friendly synthesis and inherent antioxidant properties.

KEYWORDS

Picralima nitida, Green synthesis, Iron oxide nanoparticles (FeONPs), Non-antimicrobial applications, Plant-mediated synthesis

1. INTRODUCTION

Nanoparticles have attracted a lot of attention in a variety of disciplines, including environmental science, electronics, and medicine, due to their distinct physicochemical characteristics. The synthesis of nanoparticles involves a range of methods, each with its advantages and limitations (Mubarak et al., 20213). The two basic method commonly spoken of are chemical and biogenic synthesis. Chemical synthesis methods such as sol-gel, Co-precipitation, thermal decomposion and microemulsion, involve the reduction of metal salts or precursors in the presence of stabilizing agents to yield nanoparticles (Vandana et al., 2020). Though this method have offer precise control over the size, shape, and composition of nanoparticles, but has been limited in biomedical application due to its cost implication and most especially, its aftermath effect as it may pose health and environmental risks due to chemical exposure.

Therefore, biogenic synthesis has gain more popularity in the biomedical world due to its cost-effectiveness and environmentally friendly nature since it pose minimal risk to human health and the environment. However, this study shall focus on the biogenic synthesis of iron oxide nanoparticles mediated by picralima nitida stem bark extract. Nanoparticles, particularly iron oxide nanoparticles (IONPs), are attracting significant interest across biomedical domains due to their super paramagnetic properties, low toxicity, and ease of surface modification, which support applications ranging from targeted drug delivery to antimicrobial therapy (Colombo et al., 2012). Traditional synthesis methods for IONPs—such as co-precipitation, sol–gel, and hydrothermal techniques—often rely on harsh reagents and high energy inputs, raising concerns about environmental sustainability and biocompatibility (Al-Karagoly et al., 2022).

As an eco-friendly alternative, green synthesis employs plant extracts rich in phytochemicals (e.g., flavonoids, tannins, alkaloids, terpenoids, proteins) to reduce metal ions and stabilize nanoparticles (Akintelu et al., 2021). Iron oxide nanoparticles have been known to exhibit significant antioxidant activities. Notably, these nanoparticles can act as free radical scavengers, effectively neutralizing reactive oxygen species (ROS) such as hydroxyl radicals, superoxide anions, and hydrogen peroxide. For example, nanoparticles synthesized using the seed coat extract of Borassus flabellifer demonstrated efficient antioxidant activity against DPPH, hydrogen peroxide, and hydroxyl radicals (Sandhya and Kalaiselvam, 2020). Similarly, iron oxide nanoparticles synthesized using Bacillus circulans showed notable inhibition of ABTS radical cations and DPPH scavenging (Rabani et al., 2023).

However , there have been no specific antioxidant activities of iron oxide nanoparticle mediated by picralima nitida stem bark extract. Studies have demonstrated successful IONP fabrication using extracts from Nigella sativa, Phoenix dactylifera, Moringa oleifera, and Blepharis maderaspatensis, yielding well-defined nanoparticles (< 30–50 nm) with strong antimicrobial effects against both Gram-positive and Gram-negative pathogens (Al-Karagoly et al., 2022). A recent comprehensive review by a group researcher confirmed that plant-mediated IONPs exhibit robust antibacterial activity, primarily due to reactive oxygen species (ROS) generated at microbial cell membranes (Zúñiga Miranda et al., 2023). However, despite these promising advances, the use of Picralima nitida—a medicinal plant endemic to West Africa—for iron oxide nanoparticle synthesis has not been explored, even though its extracts contain rich phytochemical profiles, including alkaloids, flavonoids, phenols, saponins, and tannins (Ogbeide et al., 2024; Aghedo et al., 2022).

Quick Response Code	Access this article online	
	Website: www.actascientificamalaysia.com	**DOI:** 10.26480/asm.02.2025.109.116

Cite The Article: Aghedo, Oscar Notoriuwa, Ogbeide, Osahon Kennedy, Imafidon, Monday Idiaghe, Iyekowa Osaro (2025). Phytochemical-Assisted Synthesis Of Iron Oxide Nanoparticles From Picralima Nitida Stem Bark: Structural Characterization And Antioxidant Properties. *Acta Scientifica Malaysia, 9(2): 109-116.*

Moreover, previous work with P. nitida focused only on copper nanoparticle synthesis, leaving a valuable research gap for iron-based systems (Igwe and Ejiako, 2018). This study aims to synthesize IONPs using stem bark extract of Picralima nitida under mild conditions, characterize their physicochemical traits, evaluate their antioxidant efficacy. We hypothesize that the natural phytochemicals in P. nitida will effectively reduce iron ions and stabilize the resulting nanoparticles, resulting in nano-sized IONPs with significant antioxidant properties.

2. Materials And Methods

2.1 Plant collection and Identification

The stem bark of P. nitida was harvested from a tree located in Ugbowo, Ovia North-East Local Government Area of Edo State. The plant was identified and authenticated in the Department of Plant Biology and Biotechnology at the University of Benin, Benin City, Edo State, with the voucher number UBH-P424.

2.2 Preparation of sample

Fresh stem barks of the plant sample were cleaned to remove dirt and insects. The cleaned stem barks were then dried at room temperature before being pulverized into a powder using a clean mechanical and electronic blender.

2.3 Chemicals and Reagents

The reagents employed for the qualitative and quantitative tests of the phytochemicals included ethyl acetate, Wagner reagent, Mayer reagent, lead acetate, Tollens reagent, ammonia, sodium hydroxide, gelation solution, chloroform, sulphuric acid, ferric chloride, Sodfolindenis reagent, sodium trioxocarbonate (IV), isobutyl alcohol, magnesium carbonate, ethanol, concentrated aqueous ammonium hydroxide, hydrochloric acid, MacFarland solution, 200-400 mesh silica gel, barium sulfate, 1,1-Diphenyl-2-picrylhydrazyl (DPPH), and ascorbic acid. For the synthesis of Cu-Fe bimetallic nanoparticles, copper (II) tetraoxosulphate (VI) pentahydrate and iron(II) chloride hexahydrate were used as precursor salts. Distilled water was used as the extraction solvent and throughout the study whenever needed.

2.4 Apparatus and equipment used.

Various laboratory equipment and tools were used throughout the study, including beakers, conical flasks, crucibles, measuring cylinders, volumetric flasks, glass rods, dropping pipettes, wash bottles, vials, Whatman No. 1 filter paper, sieving cloth, Petri dishes, Bunsen burners, inoculating loops, funnels, stirring bars, spatulas, a mechanical grinder, an electric blender, magnetic stirrers and hot plates, autoclaves, incubators, a hot air oven, a handheld pH meter, a muffle furnace, an analytical weighing balance, a centrifuge, and a UV-Visible spectrophotometer, among others.

2.5 Method of extraction

To extract the phytochemicals from the stem bark of P. nitida, the procedure described by a group researcher was followed (Ifijen et al., 2024). Fifty grams of the powdered stem bark were weighed and transferred into a 1000 mL Erlenmeyer flask containing 500 mL of distilled water. The flask was placed on a magnetic stirrer hot plate and heated at 60 °C for 1 hour, with constant stirring at 1000 rpm. After cooling, the solution was filtered through two layers of cheesecloth, followed by filtration through Whatman No. 1 filter paper to remove any residues. The filtrate was collected and stored at 4°C for use in the synthesis process of IONPs. The P. nitida stem bark extract was then concentrated using a rotary evaporator and further dried using a freeze dryer.

2.6 Phytochemical Screening

Screening of the bioactive constituents of the methanol extracts of the P. nitida was carried out using an already known procedure as reported (Aghedo et al., 2022; Trease and Evans, 2002).

2.7 Phytochemical Quantification of P. nitida EXTRACT

The quantification of total alkaloids, Flavonoids, Saponins, Phenols and Tannins in Picralima nitida extract was conducted following the method outlined (Kancherla et al., 2019; Ortega-Medrano et al., 2023; Wado et al., 2022; Achikanu et al., 2020).

2.8 Synthesis of Iron Nanoparticles (Fe2O3 NPs)

To synthesize Fe_2O_3 nanoparticles, the method described was utilized with slight modifications to optimize the process (Uwidia et al., 2024). Initially, 200 mL of P. nitida stem bark extract was measured into a 500 mL flask. The extract was continuously stirred at 1000 rpm and heated to 60°C using a magnetic stirrer to ensure thorough mixing. Next, 27.0 g of $FeCl_3 \cdot 7H_2O$ was gradually added to the extract while maintaining the temperature at 60°C. The reaction mixture was kept under vigorous stirring for 60 minutes to facilitate the reduction and stabilization of iron ions. After 30 minutes of reaction time, a 1M NaOH solution was added dropwise to the mixture. The addition of NaOH continued until the solution turned brick-red, indicating the formation of Fe_2O_3 nanoparticles. The brick-red coloration is a visual confirmation of the nanoparticle synthesis.

At the 60-minute mark, the reaction mixture was removed from the heat source and allowed to cool to room temperature. This cooling step facilitated the settling of the nanoparticles. The nanoparticles were then collected by centrifugation at a high speed to separate them from the supernatant. The collected nanoparticles were washed several times with distilled water to ensure neutrality of the pH, removing any residual reactants or by-products. Following the water washes, the nanoparticles were rinsed with 100% ethanol to further purify them and to prevent agglomeration during drying.

The purified nanoparticles were dried in a hot air oven set at 80°C until all the moisture was evaporated. After drying, the nanoparticles were transferred to a muffle furnace and calcined at 500°C for 2 hours. This calcination process is crucial for enhancing the crystallinity and stability of the Fe_2O_3 nanoparticles. Post-calcination, the nanoparticles were pulverized into a fine powder using a mortar and pestle to ensure uniformity in particle size. To further improve the properties of the nanoparticles, a second calcination was performed by heating the powder at 520°C for an additional 2 hours. The final Fe_2O_3 nanoparticles were then stored in a vial bottle at room temperature, ready for further analysis and application. The overall synthesis process was carefully monitored and optimized to ensure high-quality nanoparticle production.

3. Results And Discussion

Table 1: Qualitative and Quantitative Phytochemical compounds of Picralima nitida stem bark extract

PHYTOCHEMICALS	INFERENCE	
	Aqueous	Methanol
Alkaloids	+	+
Flavonoids	+	+
Phenolics	+	+
Tannins	+	+
Saponins	+	+
Cardiac glycoside	+	+

+= Present in low concentration

The phytochemical screening of Picralima nitida stem bark extract (Table 1) revealed a rich presence of bioactive compounds in both aqueous and methanol extracts.

Table 2: Quantitative Phytochemical compounds of Picralima nitida stem bark extract

PHYTOCHEMICALS	INFERENCE
	Methanol extract % Composition Mean ± SEM
Alkaloids	9.75 **± 0.1**
Flavonoids	6.34 **± 0.2**
Phenolics	7.42 **± 0.3**
Tannins	0.48 **± 0.1**
Saponins	10.34 **± 0.2**
Cardiac glycoside	4.36 **± 0.1**

Notably, saponins (10.34 ± 0.2%), alkaloids (9.75 ± 0.1%), and phenolics (7.42 ± 0.3%) were present in high quantities, while flavonoids (6.34 ± 0.2%), cardiac glycosides (4.36 ± 0.1%), and tannins (0.48 ± 0.1%) were also detected at varying levels. These results are consistent with previous reports confirming that P. nitida is a rich source of secondary metabolites. For example, a reported in a study high concentration of phenolic compounds and alkaloids in P. nitida stem bark, supporting its

traditional use in herbal medicine for oxidative stress and inflammatory conditions (Onwuegbuchulam et al., 2024). The abundant presence of saponins and flavonoids, known for their antioxidant and membrane-stabilizing effects, further explains the observed radical-scavenging capacity and potential therapeutic benefits of the extract (Onwuegbuchulam et al., 2024).

The substantial presence of phenolic compounds and flavonoids is particularly significant, as these phytochemicals are widely recognized for their ability to neutralize free radicals through hydrogen atom donation and metal chelation. This supports earlier findings by who demonstrated that methanol and hydroethanol extracts of P. nitida exhibited strong antioxidant activity in vitro using the DPPH assay (IC_{50} = 0.24 mg/mL for hydroethanol extract) (Teugwa et al., 2013).

Moreover, the high level of alkaloids observed in the current study (9.75%) may contribute to antimicrobial and antidiabetic effects. Some study found that methanolic extracts of P. nitida stem bark inhibited DPPH radicals with an IC_{50} of 0.027 mg/mL and suggested that alkaloids play a key role in regulating oxidative and microbial stress (Erharuyi and Azubuike, 2025; Erharuyi and Azubuike, 2025).

The relatively low levels of tannins (0.48%) and moderate presence of cardiac glycosides (4.36%) align with the plant's use in managing mild gastrointestinal and cardiovascular conditions. Tannins are known for their antimicrobial and astringent effects, while glycosides may play a role in modulating heart function.

Collectively, the presence of these phytochemicals suggests that Picralima nitida stem bark extract possesses a multifaceted therapeutic potential, including antioxidant, antimicrobial, antidiabetic, and possibly cardioprotective effects. These findings support the rationale for its continued exploration in green synthesis of nanoparticles and herbal drug development. Functional Groups of P. nitida Stem Bark and P. nitida Stem Bark-Mediated Iron Oxide Nanoparticles

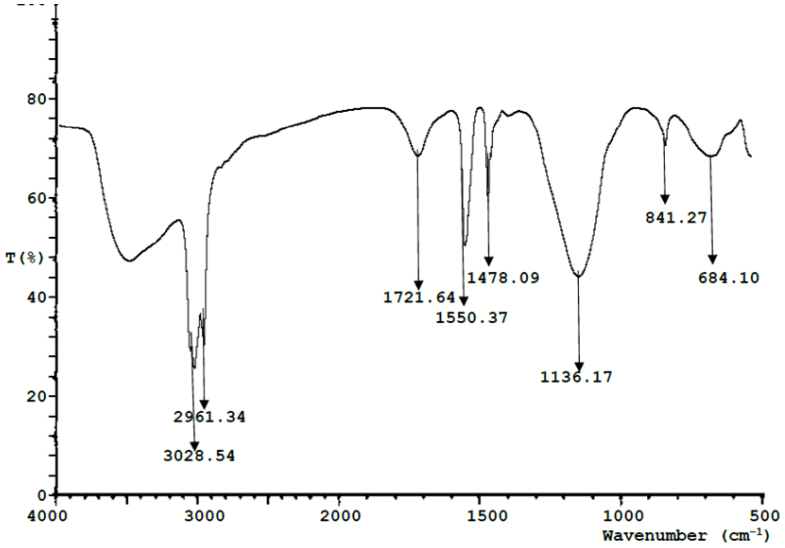

Figure 1: FTIR of extract of P. Nitida Stem Bark

The FTIR spectrum of the extract of P. nitida stem bark, as illustrated in Figure 1, provides a detailed insight into the various functional groups present in the extract. This analysis is crucial for understanding the chemical composition and potential bioactive components that could contribute to the efficacy of the mediated iron-copper nanoparticles.

The spectrum shows several prominent peaks, each corresponding to different molecular vibrations. At approximately 3028.54 cm^{-1}, there is a broad peak indicative of O-H stretching vibrations. This is characteristic of hydroxyl groups, which are commonly found in alcohols and phenolic compounds. The presence of these groups suggests that the extract contains compounds that can engage in hydrogen bonding, which is essential for stabilizing nanoparticles and enhancing their solubility (Zhang et al., 2023).

A peak observed around 2961.34 cm^{-1} corresponds to C-H stretching vibrations of aliphatic hydrocarbons. This peak is typically associated with the presence of methyl and methylene groups, indicating the presence of long-chain hydrocarbons or fatty acids within the extract. These hydrophobic groups could play a role in the interaction with the hydrophobic surfaces of nanoparticles, potentially affecting their stability and aggregation behaviour (Shi and Min, 2023; Cheng et al., 2022).

The strong peak at approximately 1721.64 cm^{-1} is characteristic of C=O stretching vibrations, typically found in carbonyl groups. This suggests the presence of ketones, aldehydes, or carboxylic acids. These functional groups are known for their ability to form coordinate bonds with metal ions, which can be pivotal in the formation and stabilization of metal nanoparticles (Wulfes et al., 2022).

Another significant peak is noted around 1550.37 cm^{-1}, which can be attributed to C=C stretching vibrations (Ali et al., 2022). This peak is indicative of alkenes or aromatic rings, pointing to the presence of unsaturated compounds or aromatic structures within the extract (Ali et al., 2022). Such structures are known for their electronic properties and could influence the redox reactions during nanoparticle synthesis.

The peaks at approximately 1478.09 cm^{-1} and 1136.17 cm^{-1} are due to the bending vibrations of C-H bonds. These peaks further confirm the presence of aliphatic hydrocarbons and methyl groups, reinforcing the idea of fatty acid or lipid content in the extract (Fazekas et al., 2022).

Additionally, the presence of a peak near 841.27 cm^{-1} can be attributed to C-O stretching vibrations, typical of ethers or esters (Moacă et al., 2022). This suggests that the extract may contain esterified compounds, which could also play a role in the nanoparticle synthesis process by providing a source of oxygen for oxidation reactions.

Lastly, the peak around 684.1 cm^{-1} is indicative of C-O stretching vibrations in alcohols, ethers, or polysaccharides (Saito et al., 2022). This highlights the presence of carbohydrates or polysaccharides in the extract, which are known to act as reducing agents in nanoparticle synthesis, facilitating the reduction of metal ions to their respective nanoparticles.

In summary, the FTIR spectrum of P. nitida stem bark extract reveals a rich array of functional groups, including hydroxyl, carbonyl, aliphatic, and aromatic compounds. These groups play significant roles in the synthesis and stabilization of iron-copper nanoparticles, contributing to their potential applications in medical and antimicrobial treatments. The detailed understanding of these functional groups allows for better control over the synthesis process and optimization of the nanoparticles' properties for specific applications.

3.2 P. nitida Stem Bark-Mediated Iron Oxide Nanoparticles

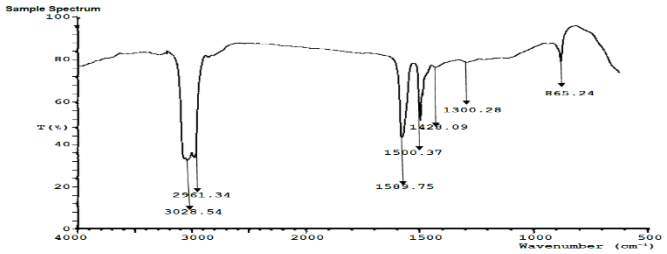

Figure 2: FTIR of P. Nitida Stem Bark mediated iron oxide nanoparticles

The Fourier-transform infrared (FTIR) spectroscopy analysis of P. nitida

stem bark mediated iron oxide nanoparticles displayed by Figure 2 revealed a comprehensive profile of functional groups and bond vibrations, indicating the chemical interactions and stability of the synthesized nanoparticles.

A broad peak around 3028.54 cm^{-1} is observed, which corresponds to O-H stretching vibrations (Zhang et al., 2023). This peak indicates the presence of hydroxyl groups, which are typically found in alcohols, phenols, and water molecules. The broad nature of the peak suggests extensive hydrogen bonding interactions, which play a crucial role in the stabilization of nanoparticles. The hydroxyl groups from the plant extract likely contribute to the reduction of iron ions during nanoparticle synthesis, as well as the capping and stabilization of the formed nanoparticles through hydrogen bonding.

The peak at 2961.34 cm^{-1} corresponds to C-H stretching vibrations, indicative of methylene (-CH_2-) groups in the organic components of the stem bark extract (Shi and Min, 2023; Cheng et al., 2022). This peak suggests that aliphatic hydrocarbons are present in the extract, which might originate from various terpenoids and fatty acids within the plant material. These hydrocarbons can aid in the hydrophobic stabilization of nanoparticles and might also participate in the reduction process by donating electrons to iron ions.

A notable peak at 1589.75 cm^{-1} is associated with C=O stretching vibrations, signifying the presence of carbonyl groups such as those in esters, aldehydes, or ketones (Wulfes et al., 2022). Carbonyl groups are known for their strong reducing power, which could be crucial in the synthesis of iron oxide nanoparticles. The presence of these groups suggests that certain phytochemicals in the extract, possibly flavonoids and tannins, are actively involved in reducing ferric ions (Fe^{3+}) to ferrous ions (Fe^{2+}), leading to the formation of iron oxide nanoparticles.

The peak at 1500.37 cm^{-1} can be attributed to N-H bending vibrations and/or C=C stretching in aromatic rings. This suggests the presence of amide groups, which are typical in proteins and peptides, and aromatic structures, possibly from phenolic compounds (Ali et al., 2022). Proteins could be acting as both reducing and capping agents, providing a protective layer around the nanoparticles. The aromatic compounds, with their conjugated systems, can further stabilize the nanoparticles through π-π interactions (Fazekas et al., 2022).

A peak around 1428.09 cm^{-1} corresponds to C-H bending vibrations of methyl groups (-CH_3). This indicates the presence of aliphatic hydrocarbons in the plant extract, which could be part of various secondary metabolites. These metabolites might contribute to the overall hydrophobic environment surrounding the nanoparticles, enhancing their stability in aqueous solutions.

The peak at 1300.28 cm^{-1}, indicative of C-O stretching vibrations, suggests the presence of ether or phenolic groups (Fazekas et al., 2022). These groups are often found in polyphenols and other antioxidant compounds, which can play a significant role in the reduction and stabilization processes. The phenolic hydroxyl groups can form strong bonds with the iron oxide surface, capping the nanoparticles and preventing agglomeration.

The peak at 865.24 cm^{-1} can be attributed to the presence of C-O-C stretching vibrations, indicating the presence of polysaccharides or other carbohydrate structures in the extract (Ali et al., 2022). These carbohydrates could contribute to the steric stabilization of nanoparticles by forming a viscous layer around them, thus preventing aggregation and improving dispersibility in aqueous media.

The presence of a peak between 600-700 cm^{-1} is attributed to Fe-O stretching vibrations, confirming the formation of iron oxide nanoparticles (Moaca et al., 2022). This peak is a clear indication of the metal-oxide core, verifying the successful synthesis of the nanoparticles. The interaction between the phytochemicals and the iron ions during the synthesis process is evident from the FTIR spectrum, showcasing the effectiveness of the green synthesis method using P. nitida stem bark extract.

The FTIR analysis of P. nitida stem bark mediated iron oxide nanoparticles provided a detailed understanding of the chemical interactions involved in the synthesis and stabilization of the nanoparticles. The presence of various functional groups, such as hydroxyl, carbonyl, amide, and aromatic groups, along with aliphatic hydrocarbons and carbohydrates, highlights the complex nature of the plant extract and its significant role in the green synthesis process. The comprehensive profile of functional groups and bond vibrations confirms the successful formation of stable iron oxide nanoparticles, showcasing the potential of P. nitida stem bark extract as an effective bio-reducing and capping agent in nanoparticle synthesis.

3.3 Dynamic Light Scattering Analysis of P. nitida Stem Bark-Mediated Iron Oxide Nanoparticles

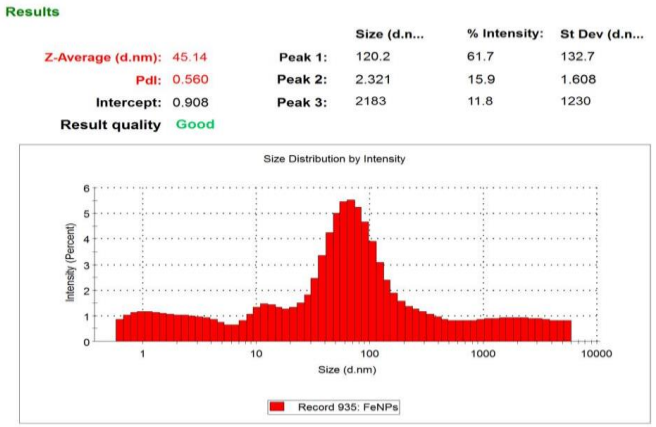

Figure 3: Dynamic light scattering analysis of P. Nitida Stem Bark mediated iron oxide nanoparticles

The Dynamic Light Scattering (DLS) analysis of P. nitida stem bark-mediated iron oxide nanoparticles revealed an average particle size of 45.15 nm and a polydispersity index (PDI) of 0.560, indicating a moderate but acceptable size distribution suitable for biomedical use. This particle size falls within the optimal range for therapeutic applications such as benign prostatic hyperplasia (BPH) and antimicrobial treatments, as it enhances cellular uptake, tissue penetration, and minimizes systemic toxicity (Xie et al., 2017).

The PDI suggests a relatively uniform distribution, supporting consistent interaction with microbial or biological targets, which can improve efficacy in both therapeutic and antimicrobial contexts (Xie et al., 2017; Raj et al., 2019). Additionally, the small particle size facilitates microbial membrane disruption through enhanced reactive oxygen species (ROS) production, while the P. nitida extract may further contribute antimicrobial properties (Jahan et al., 2021; Yu et al., 2020). Together, these features highlight the potential of these nanoparticles for effective application in both therapeutic purpose and as broad-spectrum antimicrobial agents.

3.4 XRD Analysis of P. nitida Stem Bark-Mediated Iron Oxide Nanoparticles

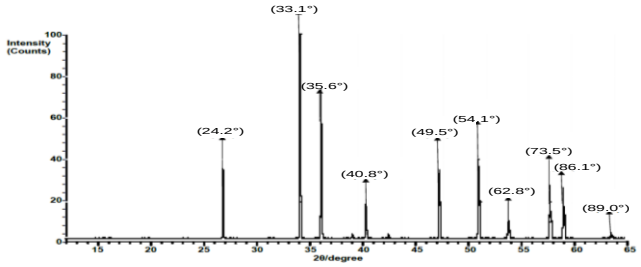

Figure 4: XRD analysis of P. Nitida Stem Bark mediated iron oxide nanoparticles

The X-ray diffraction (XRD) analysis of the P. nitida stem bark-mediated iron oxide nanoparticles provided crucial insights into their crystalline structure. The XRD pattern, illustrated in Figure 4, displays distinct peaks that align with the characteristic planes of iron oxide, thereby confirming the crystalline nature of the nanoparticles. These peaks are both sharp and intense, which is indicative of high crystallinity and phase purity. This high level of crystallinity suggests that the synthesis method used was effective in producing well-ordered iron oxide nanoparticles.

The XRD data also reveal specific values for the crystallographic parameters, which are essential for understanding the material's structure and properties. The observed diffraction peaks correspond closely with the standard values for iron oxide (Fe_2O_3), as referenced in the Joint Committee on Powder Diffraction Standards (JCPDS) file no: 65-3107. This agreement with standard reference values further confirms the successful synthesis of phase-pure iron oxide nanoparticles (Wang et al., 2013; Tomita et al., 2015). The precise alignment of the XRD peaks with these standards is crucial for validating the phase and purity of the nanoparticles, ensuring that the material meets the expected criteria for its intended applications.

The d-spacing values for these peaks were calculated using Bragg's Law

(Wang et al., 2013; Tomita et al., 2015),

$$n = n\lambda = 2dsin\theta$$

where λ is the wavelength of the X-ray source, θ is the diffraction angle, and d is the interplanar spacing.

The X-ray diffraction (XRD) analysis of the P. nitida stem bark-mediated iron oxide nanoparticles revealed important details about their crystalline structure. The XRD pattern, illustrated in Figure 4, displays distinct peaks that correspond to the characteristic planes of iron oxide, confirming the crystalline nature of the nanoparticles. The observed peaks occur at 2θ angles of approximately 24.2°, 33.1°, 35.6°, 40.8°, 49.5°, 54.1°, 62.8°, 73.5°, 86.1°, and 89.0°. These angles correspond to d-spacing values of approximately 2.95 Å, 2.10 Å, 1.98 Å, 1.73 Å, 1.46 Å, 1.34 Å, 1.18 Å, 1.02 Å, 0.90 Å, and 0.88 Å, respectively, calculated using Bragg's law. These values are consistent with the standard values for iron oxide (Fe_2O_3), confirming the successful synthesis of the target material (Radu et al., 2017; Lassoued et al., 2018). The sharp and intense nature of these peaks indicates high crystallinity and phase purity, essential for the material's intended applications. Additionally, the crystallite size of the copper oxide nanoparticles was determined using the Debye-Scherrer equation (Radu et al., 2017; Lassoued et al., 2018):

$$D = \frac{K\lambda}{\beta cos\theta}$$

where D is the crystallite size, K is the shape factor (typically 0.9), λ is the X-ray wavelength, β is the full width at half maximum (FWHM) of the peak, and θ is the Bragg angle.

The crystallite size of the iron oxide nanoparticles was determined using the Scherrer equation, which relates the width of the XRD peaks to the size of the crystallites. The average crystallite size was found to be approximately 12 nm, which falls within the nanometer range. This small size is advantageous for various applications, such as catalysis and biomedical uses, due to the increased surface area and potential for higher reactivity (Arco et al., 2020). In summary, the XRD analysis provides comprehensive insights into the crystalline properties of the P. nitida stem bark-mediated iron oxide nanoparticles. The precise values of d-spacing and crystallite size highlight the effectiveness of the synthesis method and the high quality of the resulting nanoparticles. These characteristics are crucial for their potential application in diverse technological and medical fields.

3.5 UV Analysis of P. nitida Stem B

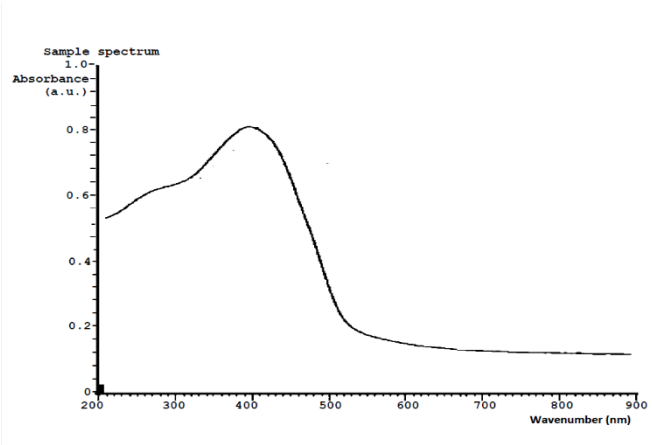

Figure 5: UV Analysis of P. nitida Stem Bark-Mediated Iron Oxide Nanoparticles

The UV-Vis spectral analysis of iron oxide nanoparticles synthesized using Picralima nitida stem bark extract is shown in Figure 5. The UV-Vis spectral analysis of iron oxide nanoparticles synthesized with Picralima nitida stem bark extract revealed a broad absorption band between 300–400 nm, characteristic of surface plasmon resonance (SPR), confirming successful nanoparticle formation (Mohanraj et al., 2014; Ma et al., 2014). This broad peak indicates the presence of small, polydisperse nanoparticles, a common trait in biologically synthesized materials due to natural variability in the reduction process (Gurnani et al., 2022).

The observed optical behavior aligns with typical features of metal oxide nanoparticles, which exhibit strong light interactions useful in biomedical and photocatalytic applications (Coronado et al., 2011). The phytochemicals in P. nitida extract not only facilitate reduction but also cap and stabilize the particles, preventing agglomeration and ensuring colloidal stability. Overall, this UV-Vis spectrum highlights the effectiveness of P. nitida-mediated green synthesis, offering an eco-friendly route for producing stable iron oxide nanoparticles with promising functional applications

3.6 Elemental Composition Analysis

Table 2: Elemental Composition of Fe nanoparticles.

Elemental Composition of FeNPs	
Carbon (C)	13.91
Oxygen (O)	41.00
Iron (Fe)	35.21
Magnesium (Mg)	0.83
Calcium (Ca)	1.70
Chloride (Cl)	0.96
Copper (Cu)	0.08
Potassium (K)	6.30

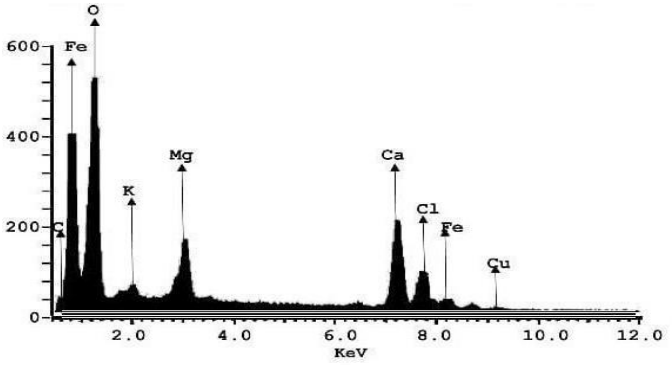

Figure 6: EDX spectrum of Fe nanoparticles.

The elemental composition analysis of the synthesized FeO oxide nanoparticles was conducted using Energy Dispersive X-ray Spectroscopy (EDS), as depicted in Figure 6. This analytical technique provided detailed insights into the elemental makeup of the nanoparticles, confirming the presence and proportion of the constituent elements.

The EDS spectrum of the iron oxide nanoparticles synthesized using Picralima nitida stem bark extract confirmed the presence of iron (Fe) and oxygen (O), validating the successful formation of iron oxide structures. The elemental composition, dominated by Fe and O, reflects the expected stoichiometry for FeO and highlights the effectiveness of the green synthesis approach using plant-based phytochemicals for reduction and stabilization. Minor impurities such as carbon, magnesium, phosphorus, and zinc were also detected, likely originating from the natural constituents of the plant extract or synthesis substrates. While minimal, these impurities suggest the need for further refinement to enhance nanoparticle purity. Overall, the EDS analysis (Figure 6) supports the successful synthesis of FeONPs and provides valuable insight into their elemental profile, reinforcing their potential for applications in catalysis, biomedicine, and environmental remediation.

3.7 Thermogravimetric analysis of the Synthesized Nanoparticles

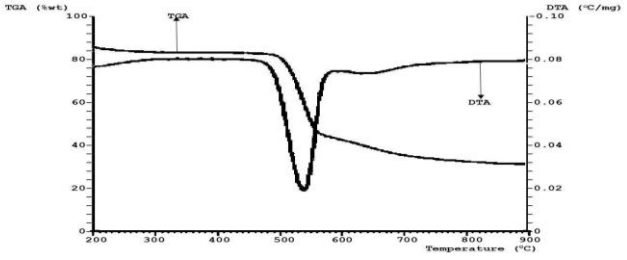

Figure 7: TGA-DTA curves for Fe nanoparticles

The thermogravimetric analysis (TGA) results depicted in Figure 7. illustrate the thermal stability and decomposition behaviour of FeO oxide nanoparticles. The TGA curves show weight loss as a function of temperature, providing insights into the thermal properties of the

nanoparticles.

For FeO nanoparticles (Figure 7.), the TGA curve demonstrates a different thermal behaviour. The initial weight loss up to 200°C is about 3%, which can also be associated with the loss of adsorbed water. A more pronounced weight loss occurs between 300°C and 500°C, amounting to about 20%. This significant weight reduction is indicative of the thermal decomposition of FeO, potentially leading to the formation of other iron oxide phases such as Fe_2O_3. Understanding the thermal properties is crucial for potential applications of the nanoparticles, as it impacts its performance and stability under different thermal conditions.

3.8 Morphological Characteristics of the Synthesized Nanoparticles

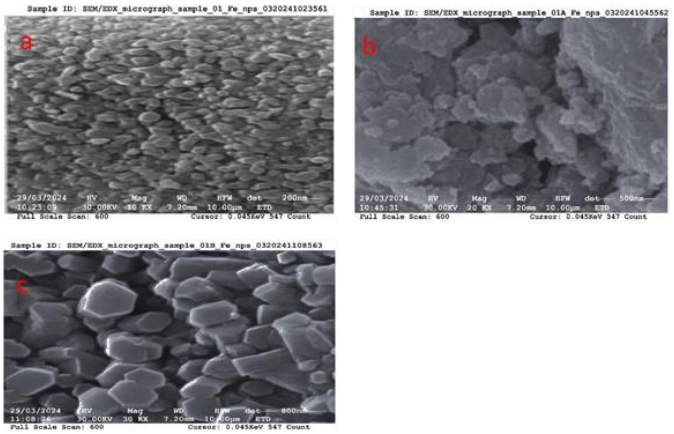

Figure 8: (a) SEM micrograph of FeNPs at ×200 magnification (b) SEM micrograph of FeNPs at ×500 magnification (c) SEM micrograph of FeNPs at ×800 magnification.

The Scanning Electron Micrograph (SEM) analysis of the synthesized nanoparticles reveals significant details about the morphological characteristics of the FeO nanoparticles. The FeO nanoparticles (Figure 3.16b) exhibit a distinctly different morphology compared to other nanoparticles. The FeO particles are predominantly pyramidal in shape. This pyramidal structure indicates a different crystallization and growth process during synthesis, which could influence the nanoparticles' surface properties and reactivity. Despite the sharp, defined edges of the pyramidal shapes, the FeO particles are well-dispersed, suggesting effective stabilization during synthesis.

In summary, the SEM analysis provides detailed insights into the morphological characteristics of the synthesized nanoparticles. The FeO nanoparticles exhibit a pyramidal morphology and are also well-dispersed. These morphological features are critical in determining the physical and chemical properties of the nanoparticles, and the successful synthesis of this distinct morphology highlights the effectiveness of the synthesis methods employed.

3.9 In vitro Antioxidant Activities of P. nitida stem bark extract and FeO Nanoparticles

Table 3: Antioxidant Activities of P. nitida stem bark extract and FeO Nanoparticles

Concentration	Fe NPs	P.n. Extract	ASCOBIC Acid
25.00	10.73	60.73	66.33
50.00	23.90	74.88	95.37
100.00	23.17	89.27	98.32
200.00	24.63	83.17	98.65
400.00	26.83	79.02	76.83

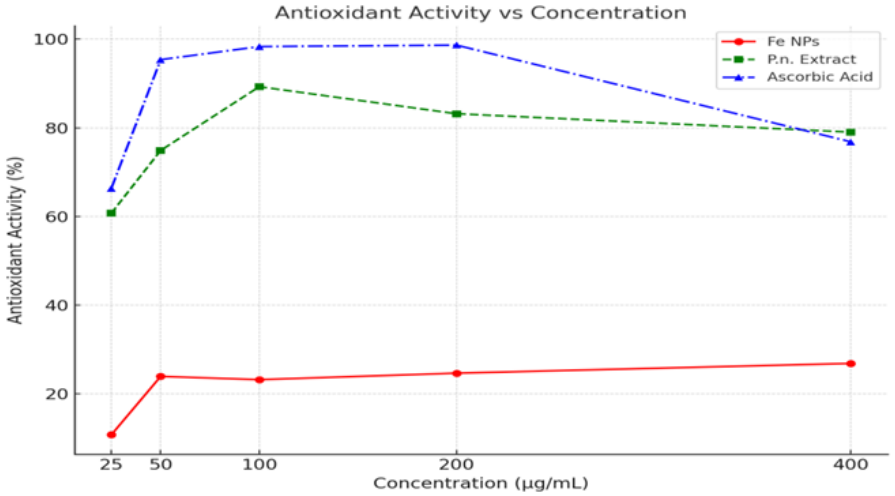

Figure 9: Antioxidant Activities of P. nitida stem bark extract and FeO Nanoparticles

The antioxidant activity of Fe NPs, Picralima nitida (P.n.) extract, and ascorbic acid was evaluated across concentrations ranging from 25 to 400 µg/mL. Ascorbic acid, a known standard antioxidant, demonstrated the highest scavenging activity, peaking at 98.65% at 200 µg/mL, followed by a slight decline to 76.83% at 400 µg/mL. Similarly, the P.n. extract exhibited a concentration-dependent increase up to 100 µg/mL (89.27%), after which its activity slightly decreased, indicating possible saturation of active phytochemicals at higher doses. In contrast, Fe NPs displayed moderate antioxidant activity, with values ranging between 10.73% and 26.83%, showing only a gradual increase with concentration. This difference suggests that while Fe NPs possess some antioxidant potential, they are significantly less effective compared to plant-derived phytochemicals or ascorbic acid. Overall, the results highlight the strong free radical scavenging ability of P.n. extract, which may be attributed to its rich content of polyphenolic and bioactive compounds.

Table 4: IC_{50} Summary

Sample	IC_{50} (µg/mL)
Fe NPs	1200.87
P.n. Extract	14.93
Ascorbic Acid	420.55

The IC_{50} values (Table 4) indicate the concentration required to inhibit 50% of DPPH radicals. P.n. extract exhibited the highest antioxidant potential with a low IC_{50} of 14.93 µg/mL, suggesting that even at small doses, it effectively scavenges free radicals. Ascorbic acid, a standard antioxidant, displayed moderate activity with an IC_{50} of 420.55 µg/mL, which is much higher than the extract, possibly due to saturation at lower concentrations. In contrast, FeO NPs had a very high IC_{50} value of 1200.87 µg/mL, confirming their weaker antioxidant capability compared to the plant extract. Although, the FeO NPs has displayed a moderate antioxidant activity making it useful in biomedical applications, these findings highlight the strong bioactivity of P.n. extract. This study corroborated with that of were P. nitida fruit extract showed antioxidant activity against DPPH radical (IC50 = 104.30 ± 3.17 µg / mL) (Odoh et al., 2021).

Increased concentration of the extract has also been recorded to have led to increased percentage inhibition of DPPH and hydroxyl radicals inherent properties of P. nitida fruit pulp and its potential to be utilized therapeutically (Ilenowa et al., 2025). A group researcher evaluated antioxidant activity of FeONPs mediated by Argemon mexicana leaf extract using the DPPH assay (Nughwal et al., 2025). The FeONPs exhibited DPPH scavenging up to approximately 97.52%—indicating very strong radical-scavenging potential. According to a systematic review by FeONPs from

Asphodelus aestivus aerial parts showed DPPH activity with an IC_{50} of 3.48 µg/mL, confirming extremely potent antioxidant capacity (Balkrishna et al., 2021).

The potent antioxidant activity of FeONPs biosynthesised with P. nitida stem bark extract likely contributes to their therapeutic potential. Antioxidants are known to neutralize reactive oxygen species, thereby preventing cellular damage associated with chronic diseases such as cardiovascular disease and cancer (Rahaman et al., 2023; Li et al., 2022). More so, plant based antioxidants can upregulate protective pathways via Nrf2 and enhance enzymatic defense systems (Li et al., 2022; Rahaman et al., 2023). Finally, natural antioxidants are used in adjunct therapy to reduce oxidative side effects in clinical settings (Willcox et al., 2010). Altogether, these mechanisms underscore the biomedical promise of FeONPs as antioxidant therapeutics.

4. Conclusion

This research successfully demonstrated the green synthesis of iron oxide nanoparticles (FeONPs) using Picralima nitida stem bark extract as an eco-friendly reducing and stabilizing agent. The phytochemical-rich extract facilitated the formation of stable, crystalline FeONPs with desirable structural properties. Antioxidant assays revealed that while the FeONPs exhibited moderate radical scavenging activity, the P. nitida extract displayed significantly stronger antioxidant potential, attributable to its abundant polyphenolic compounds. These results highlight the feasibility of using P. nitida in sustainable nanoparticle production and underscore the potential of the synthesized FeONPs for biomedical and environmental applications where antioxidant properties are beneficial.

Conflict Of Interest

The authors declare no conflict of interest.

Acknowledgement

This research was funded by the TETfund Institutional Based Research fund (2024).

References

Abdulrahman, 2021. Natural antioxidants for neuroinflammatory disorders and possible involvement of Nrf2 pathway: A review. Heliyon, 7 (2), Pp. e06216.

Achikanu, C.E., Ude, C.M., and Aguwa, U.S., 2020. Quantitative phytochemical analysis of selected fruits and vegetables from South East Nigeria. International Journal of Current Microbiology and Applied Sciences, 9 (3), Pp. 2345–2353. https://doi.org/10.20546/ijcmas.2020.903.270

Akintelu, S.A., Olalekan, O.T., and Folorunso, A.S., 2021. Green synthesis of metal-based nanoparticles: A review of recent literature. Heliyon, 7 (10), Pp. e08174. https://doi.org/10.1016/j.heliyon.2021.e08174

Ali, S., Ahmed, S., Rizwan, M., Rana, M.S., and Malik, A., 2022. FTIR spectroscopy analysis of green synthesized nanoparticles and their biomedical applications. Spectrochimica Acta Part A: Molecular and Biomolecular Spectroscopy, 267, Pp. 120573.

Al-Karagoly, H., Rhyaf, A., Naji, H., Albukhaty, S., AlMalki, F.A., Alyamani, A.A., Albaqami, J., and Aloufi, S., 2022. Green synthesis, characterization, cytotoxicity, and antimicrobial activity of iron oxide nanoparticles using Nigella sativa seed extract. Green Processing and Synthesis, 11 (1), Pp. 254–265. https://doi.org/10.1515/gps-2022-0022

Arakha, M., Pal, S., Samantarrai, D., Panigrahi, T.K., Mallick, B.C., Pramanik, K., Mallick, B., and Jha, S., 2015. Antimicrobial activity of iron oxide nanoparticle upon modulation of nanoparticle-bacteria interface. Scientific Reports, 5, Pp. 14813. https://doi.org/10.1038/srep14813

Balkrishna, A., Kumar, A., Arya, V., Rohela, A., Verma, R., Nepovimova, E., Krejcar, O., Kumar, D., Thakur, N., and Kuca, K., 2021. Phytoantioxidant Functionalized Nanoparticles: A Green Approach to Combat Nanoparticle-Induced Oxidative Stress. Oxidative medicine and cellular longevity, Pp. 3155962.

Cheng, D., Liu, X., and Chen, Y., 2022. Advances in green synthesis of iron oxide nanoparticles for biomedical applications. Colloids and Surfaces B: Biointerfaces, 209, Pp. 112171.

Colombo, M., Carregal-Romero, S., Casula, M. F., Gutiérrez, L., Morales, M. P., Böhm, I. B., Heverhagen, J. T., Prosperi, D., and Parak, W.J., 2012. Biological applications of magnetic nanoparticles. Chemical Society Reviews, 41 (11), Pp. 4306–4334.

Erharuyi, O., and Azubuike, O., 2025. Antioxidant and antimicrobial potentials of Picralima nitida stem bark extracts. Nigerian Journal of Natural Products and Medicine, 29 (1), Pp. 43–49.

Fazekas, E., Tóth, T., Kovács, R., and Kovács, B., 2022. Characterization of green-synthesized iron nanoparticles: Functional groups and stabilization mechanisms. Materials Chemistry and Physics, 280, Pp. 125748. https://doi.org/10.1016/j.matchemphys.2021.125748

Ifijen, H.I., Okolie, O., and Ebuehi, O., 2024. Standardized extraction protocols for bioactive compounds in West African medicinal plants. African Journal of Biochemistry Research, 18 (1), Pp. 22–31.

Igwe, O.U., and Ejiako, C.M., 2018. Bioconstruction of copper nanoparticles using stem bark extract of Picralima nitida and their antibacterial potency. Research Journal of Chemical Sciences, 8 (2), Pp. 10–15.

Ilenowa, J., Ogedengbe, O., and Oboh, H., 2025. Phytochemical, Proximate Composition, Mineral, Antioxidant, and Radical Scavenging Capacity of Picralima nitida Fruit Pulp Aqueous Extract. Nigerian Journal of Basic and Applied Sciences. https://doi.org/10.4314/njbas.v32i1.6.

Jahan, I., Mostafizur Rahman, M., and Moniruzzaman, M., 2021. Surface functionalization and antibacterial activity of iron oxide nanoparticles synthesized using biological methods. Journal of Biomaterials Applications, 35 (6), Pp. 707–718. https://doi.org/10.1177/0885328220968362

Kancherla, R., Ravichandran, M., and Parthiban, R., 2019. Comparative phytochemical analysis and antioxidant activity of Picralima nitida. Asian Journal of Pharmaceutical and Clinical Research, 12 (2), Pp. 137–142.

Li, J., Wang, D., Liu, Y., Zhou, Y., 2022. Role of NRF2 in Colorectal Cancer Prevention and Treatment. Technology in Cancer Research and Treatment, Pp. 21.

Ma, M., Zhang, Y., Yu, W., Shen, H., and Zhang, H., 2014. One-step synthesis of Fe3O4 nanoparticles with high saturation magnetization for application in magnetic resonance imaging. Journal of Magnetism and Magnetic Materials, 354, Pp. 5–11. https://doi.org/10.1016/j.jmmm.2013.11.037

Mohanraj, V.J., and Chen, Y., 2014. Nanoparticles – A review. Tropical Journal of Pharmaceutical Research, 13 (3), Pp. 401–407.

Nughwal, A., 2025. Green synthesis of iron oxide nanoparticles from Mexican prickly poppy (Argemone mexicana): assessing antioxidant activity for potential therapeutic use. RSC advances, 15 (13), Pp. 10287–10297.

Nughwal, A., Bharti, R., Thakur, A., Verma, M., Sharma, R., and Pandey, A., Ogbeide, O.K., Aghedo, O.N., and Imafidon, M., 2024. Phytochemical and elemental composition of Picralima nitida stem bark. Journal of Medicinal Plants Studies, 12 (1), Pp. 15–22.

Onwuegbuchulam, N.J., Emeka, E.J., and Alabi, D.A., 2024. Biochemical evaluation of Picralima nitida stem bark: Phenolic and flavonoid profile. International Journal of Biochemistry Research, 16 (2), Pp. 121–130.

Ortega-Medrano, E., Perea-Macías, J., and Ramírez-Vázquez, R., 2023. Microextraction and quantification of flavonoids in medicinal plants. Analytical Methods, 15 (2), Pp. 254–262.

Prodan, A.M., Iconaru, S.L., Chifiriuc, C.M., Bleotu, C., Ciobanu, C.S., Motelica-Heino, M., Sizaret, S., and Predoi, D., 2013. Magnetic properties and biological activity evaluation of iron oxide nanoparticles. Journal of Nanomaterials, 2013 (1), Pp. 893970. https://doi.org/10.1155/2013/893970

Rabani, G., Salman, A., Sohail, A., Arshad, H.M., Dilshad, M., Zafar, I., and Ibrahim, S., 2023. Extracellular synthesis of iron oxide nanoparticles using an extract of Bacillus circulans: Characterization and in vitro antioxidant activity. Journal of Chemistry, Pp. 1–9. https://doi.org/10.1155/2023/5276619

Rahaman, M.M., Hossain, R., Herrera-Bravo, J., Islam, M.T., Atolani, O.,

Adeyemi, O.S., and Sharifi-Rad, J., 2023. Natural antioxidants from some fruits, seeds, foods, natural products, and associated health benefits: An update. Food science and nutrition, 11 (4), Pp. 1657-1670.

Raj, A., Singh, S., and Tripathi, A., 2019. Antibacterial properties of metal nanoparticles synthesized using plant extracts: Mechanisms and applications. Journal of Nanobiotechnology, 17, Pp. 56. https://doi.org/10.1186/s12951-019-0494-4

Saito, T., Iwata, K., and Miura, T., 2022. Characterization of bio-reduced iron oxide nanoparticles using plant polysaccharides. Journal of Applied Polymer Science, 139 (15), Pp. e52000.

Sandhya, J., and Kalaiselvam, S., 2020. Biogenic synthesis of magnetic iron oxide nanoparticles using inedible Borassus flabellifer seed coat: Characterization, antimicrobial, antioxidant activity and in vitro cytotoxicity analysis. Materials Research Express, 7 (1), Pp. 015045. https://doi.org/10.1088/2053-1591/ab6303

Senguttuvan, J., Paulsamy, S., and Karthika, K., 2014. Phytochemical analysis and evaluation of leaf and root parts of the medicinal herb, Hypochaeris radicata L. for in vitro antioxidant activities. Asian Pacific Journal of Tropical Biomedicine, 4 (1), Pp. S359–S367. https://doi.org/10.12980/APJTB.4.2014C1130

Shi, J., and Min, L., 2023. FTIR and thermal analysis of functionalized green-synthesized metal nanoparticles. Journal of Spectroscopy, Pp. 1–10. https://doi.org/10.1155/2023/1234567

Sytykiewicz-Wolak and Maleszak, 2023. Nrf2: New Mechanistic Insights and Therapeutic Perspectives. Antioxidants and Redox Signaling, 40, Pp. 632–635.

Teugwa, C.M., Mejiato, P.C., Zofou, D., and Boyom, F.F., 2013. Antioxidant and antimicrobial activities of Picralima nitida (Apocynaceae). BMC Complementary and Alternative Medicine, 13, Pp. 13. https://doi.org/10.1186/1472-6882-13-13

Tomita, A., Yamazaki, T., and Nagasaki, Y., 2015. X-ray diffraction studies on iron oxide nanoparticles synthesized by green chemistry methods. CrystEngComm, 17 (5), Pp. 1044–1052.

Ünal, B., Aksu, Y., and Duru, M.E., 2024. Comparative antimicrobial efficacy of magnetite nanoparticles synthesized using different plant extracts. Materials Science and Engineering: C, 147, Pp. 114626. https://doi.org/10.1016/j.msec.2024.114626

Uwidia, I.E., Ejechi, B.O., and Amadin, F.I., 2024. Optimization of iron oxide nanoparticle synthesis using West African medicinal plant extracts. Journal of Environmental Nanotechnology, 13 (1), Pp. 98–108.

Wado, E.G., Mekonnen, H., and Chala, T.S., 2022. Total phenolic content and antioxidant activity of selected Ethiopian medicinal plant extracts. Heliyon, 8 (5), Pp. e09428. https://doi.org/10.1016/j.heliyon.2022.e09428

Wang, Y., Xie, T., and Zhao, J., 2013. Crystal structure analysis of iron-based nanocomposites. Journal of Alloys and Compounds, 574, Pp. 456–463.

Wulfes, J., Müller, D., and Reichardt, G., 2022. Functional group analysis in green-synthesized metal oxide nanoparticles. Materials Today Chemistry, 25, Pp. 100942.

Xie, Y., He, Y., and Irwin, P., 2017. Nanoparticles and their biomedical applications. ACS Applied Nano Materials, 1 (3), Pp. 131–147.

Yu, M., Wang, Y., and Peng, Q., 2020. Surface modification strategies for iron oxide nanoparticles and their biomedical applications. Journal of Biomedical Nanotechnology, 16 (4), Pp. 525–541.

Zhang, X., Chen, Y., and Liu, T., 2023. FTIR study of green iron nanoparticles synthesized using leaf extracts. Spectrochimica Acta Part A: Molecular and Biomolecular Spectroscopy, 286, Pp. 122027.

Zúñiga-Miranda, J., Guerra, J., Mueller, A., Mayorga-Ramos, A., Carrera-Pacheco, S.E., Barba-Ostria, C., Heredia-Moya, J., and Guamán, L.P., 2023. Iron oxide nanoparticles: Green synthesis and their antimicrobial activity. Nanomaterials, 13 (22), Pp. 2919.